EUROPEAN SOUTHERN OBSERVATORY

Organisation Européenne pour des Recherches Astronomiques dans l'Hémisphère Austral
Europäische Organisation für astronomische Forschung in der südlichen Hemisphäre

VISITING ASTRONOMERS SECTION • Karl-Schwarzschild-Straße 2 • D-85748 Garching bei München • e-mail: visas@eso.org • Tel.: +49-89-32 00 62 23

APPLICATION FOR OBSERVING TIME PERIOD: **70A**

To be submitted only to: proposal@eso.org
Important Notice:

By submitting this proposal, the PI takes full responsibility for the content of the proposal, in particular with regard to the names of COIs and the agreement to act according to the ESO policy and regulations, should observing time be granted

1. Title Panel: **B–7**

UNDERSTANDING UNUSUAL BAL QUASARS USING NEAR-IR SPECTROSCOPY

2. Abstract

It is likely that every quasar is a Broad Absorption Line quasar for at least part of its lifetime. The Sloan Digital Sky Survey has discovered several previously unrecognized categories of unusual BAL Quasars, which indicate that BAL outflows have a wider range of properties than previously thought. These extreme properties might reflect extremes in the M_{BH}–$\dot{M}/\dot{M}_{edd}$ relationship for these objects. Normal BAL quasars occupy a distinct region in the M_{BH}–$\dot{M}/\dot{M}_{edd}$ plane at low redshift. This relationship can be studied at high redshift by using FWHM(Hβ) to estimate M_{BH} where direct M_{BH} measurements are impossible. Thus we propose near-IR spectroscopy to study the M_{BH}–$\dot{M}/\dot{M}_{edd}$ relationship in unusual BAL quasars. We will also compare the broad Fe II & narrow [O III] emission properties of this small but well-defined sample to those of normal BALs, and compare the reddening of the broad emission lines and the UV continuum in several extremely reddened objects.

3.

Run	Telescope	Instrument	Time	Month	Moon	Seeing	Sky Trans.	Obs.Mode
A	NTT	SOFI	1n	oct	n	n	THN	v
B	NTT	SOFI	1n	feb	n	n	THN	v
C	UT1	ISAAC	4h	any	n	n	THN	s

4. Number of nights/hours Telescope(s) Amount of time

a) already awarded to this project:

b) still required to complete this project:

5. Special remarks

6. Principal Investigator: P. HALL (P. Universidad Catolica, RCH, phall@astro.puc.cl)

Col(s): B. WILLS (Texas, USA)

7. Is this proposal linked to the PhD thesis preparation of one of the applicants?

8. Description of the proposed programme

A) Scientific Rationale:

The ubiquity of supermassive black holes in nearby massive galaxies (Kormendy & Ho 2000), and the proportionality between M_{bh} and spheroid masses (Ferrarese & Merrit 2000; Gebhardt et al. 2000), suggests that supermassive black holes, and thus high-redshift quasars, are fundamental to galaxy evolution. It may be that in a young galaxy full of massive dusty gas clouds, near- or super-Eddington black hole accretion regulates the formation of a quasar, and via the resulting powerful winds, the parallel growth of a galaxy spheroid (e.g. Fabian 1999, Silk & Rees 1998). Some quasars have spectacular broad absorption line (BAL) troughs blueward of the strong broad resonance emission lines, indicating powerful outflows up to $\sim 0.2c$ (e.g. Hall et al. 2002). These BAL quasars, with typically reddened continua but high IR luminosities, are suggested to have extreme accretion rates relative to the Eddington limit, $\dot{M}/\dot{M}_{Edd}$. They may be young quasars, glimpsed for the first time as the dusty gas clouds in their host galaxies are dispersed (Voit et al. 1993). The very youngest quasars might be the most dust-reddened, or to have the highest column densities of low-ionization gas in their BAL regions. The Sloan Digital Sky Survey (SDSS) is finding just these sorts of objects, plus a handful of possible 'medium-ionization' objects, which may be formerly dusty low-ionization BAL quasars on their way to becoming the more common, less dusty high-ionization BAL quasars (Hall et al. 2002).

To understand these unusual BAL quasars, we need to understand how their basic physical parameters compare to those of normal BAL and non-BAL quasars. For AGN and quasars we now have a way to measure M_{bh} and $\dot{M}/\dot{M}_{Edd}$ using the luminosity and the width of the broad Hβ emission line. The M_{bh}–spheroid relationship has led to calibration of the Keplerian relationship between M_{bh} and v, the broad Hβ FWHM in km s^{-1}, for low-z AGN and quasars (Laor 1998, 2001; Lacy et al. 2001): $M_{bh}/10^9 M_\odot \sim 0.2\,(v/3000)^2\,(L_{bol}/10^{46})^{1/2}$, and $\dot{M}/\dot{M}_{Edd} = 0.4\,(v/3000)^{-2}\,(L_{bol}/10^{46})^{1/2}$, assuming Keplerian velocities and distance of line-emitting clouds $\sim 0.1\,L_{bol}^{1/2}$ pc from the center (e.g. Laor 2000, Kaspi et al. 2000), where L_{bol} ($\propto \dot{M}c^2$) is in units of erg/s. In the M_{bh} – $\dot{M}/\dot{M}_{Edd}$ plane (Fig. 1), several AGN classes are distinct. Compared with radio-quiet quasars (RQQs), the radio-loud quasars (RLQs) lie at higher M_{bh}, with a range of $\dot{M}/\dot{M}_{Edd}$. The 3 known BAL quasars at low z, with high luminosities and relatively narrow Hβ lines, appear to have the highest $\dot{M}/\dot{M}_{Edd}$, as hypothesized.

Optical spectra show striking dependences on these parameters: as $\dot{M}/\dot{M}_{Edd}$ increases, Fe II emission becomes much stronger, [O III]λ5007 much weaker, and the blue wing of broad Hβ strengthens (Figs. 2; Laor et al. 1997, Boroson & Green 1992, Boroson 2001). The inverse Fe II – [O III] relationship may be explained by dense, high column densities of low-ionization Fe II-emitting gas in the broad emission line region (BLR) preventing photons from reaching and ionizing the more distant narrow line region. Thus high $\dot{M}/\dot{M}_{Edd}$ is strongly related to the availability of this potential fuel supply, and since the SDSS may be finding the objects with the largest available fuel supplies (e.g. Fig. 3), extreme SDSS quasars provide a simple test of this hypothesis.

There are few known low-z BAL quasars because only UV rest-frame spectra can reveal the strong UV absorption troughs, and because BAL outflows are rare at low L_{bol}. In order to investigate the M_{bh} and $\dot{M}/\dot{M}_{Edd}$ of BAL quasars, Wills et al. (in prep.) therefore observed a sample of bright, well-known BAL quasars at $z \sim 1$–2. Fig. 2a shows that they extend the relationship defined by low-z AGN/quasars to extreme Fe II strength and very weak [O III], strongly suggesting extreme $\dot{M}/\dot{M}_{Edd}$. Surprisingly, Hβ in high z BAL quasars is much too broad to agree with $\dot{M}/\dot{M}_{Edd}$ relationships defined at lower z and L_{bol} (e.g. Fig. 2b). It is difficult to measure Hβ asymmetry in near IR spectra of these faint quasars, but recall that in low z samples, the strength of the Hβ blue wings increases with $\dot{M}/\dot{M}_{Edd}$. We therefore suggest that, for BAL quasars, Hβ has a non-virial contribution, perhaps emission from the outflowing BAL gas. Once again, extreme BAL SDSS quasars afford a simple test of this idea, allowing a search for such emission in objects with high column density outflows extending 13000 km s^{-1} or more blueward of the systemic redshift (e.g., Fig. 3).

B) Immediate Objective:

Recent large surveys (e.g. Becker et al. 2000) have revealed many new, spectacular BAL quasars. In particular, Hall et al. (2002) presented a sample of 23 unusual BAL quasars from early SDSS data (e.g. Figs. 3-5). The sample is not complete because not all SDSS quasar candidates in the early data have been observed spectroscopically, but it is thorough in the sense that it consists of all unusual BAL quasars from a representative spectroscopic sample. This sample affords us the opportunity to study the fundamental properties (M_{bh}, $\dot{M}/\dot{M}_{Edd}$, column densities and covering fractions of dense BLR gas) of the most extreme examples of BAL quasars – and BAL quasars are already a class of objects which sample the extremes of these properties. Thus we propose near-IR spectroscopy of all unusual BALs visible from NTT, to characterize the rest-frame optical spectral properties of these unique objects and achieve the following goals:

1. The continuum SEDs enable comparison of reddening with $\dot{M}/\dot{M}_{Edd}$: are dustier objects higher accretors?
2. The magnitudes and de-reddened spectral energy distributions will allow a determination of L_{bol} (i.e., $\propto \dot{M}c^2$).
3. The Balmer line widths combined with a de-reddened L_{bol} then allow determination of M_{bh} and $\dot{M}/\dot{M}_{Edd}$, if widths measure virial velocities (to be tested – see 5.).
4. The emission-line strengths and ratios, combined with results of 1.–3. above, will allow an investigation of the fueling of the central engine via the M_{bh}, $\dot{M}/\dot{M}_{Edd}$, and Fe II, H$\beta$and [O III] emission-line relationships discussed above. How do BAL quasars compare with non-BAL RQQs and RLQs in this parameter space? Do

8. Description of the proposed programme (continued)

our extreme BALs sample the extremely dusty and/or young tail of a distribution of youthful super accretors, or are we just by chance looking along rare high column density lines of sight which exist even in run of the mill BAL quasars?
5. (related to 3.) Observations of the Hα region are valuable. It is almost always much less blended than Hβ and is valuable for searching for profile asymmetry that would indicate radial motions in the broad emission line region. Asymmetric profiles should still enable useful constraints on Keplerian velocities.
6. We will compare the above measurements with parameters of the absorbing outflows seen in the existing high-quality SDSS (rest-frame UV) spectra, especially with the velocities and strengths of the BAL outflows.

These IR spectra will also constrain various properties of the different types of unusual BAL quasars.
Some of these BALs are so extreme that their redshifts are rather uncertain since emission lines are weak, absent, or absorbed (Figs. 3-4); in three cases, the objects might not be BALs at all (e.g. Fig. 5). If our three 'mystery objects' (0338+0056 plus 0105−0033 and 2204+0031) have strong Fe II and Balmer emission in the near-IR, they can be modeled as BAL quasars with dusty-scattering-dominated continua (Hines et al. 2001); if not, less plausible explanations must be appealed to (Hall et al. 2002).
Somewhat similarly, the mechanism producing strong Fe III absorption (but not Fe II) in some objects is not understood; rest-frame optical spectroscopy might provide clues.
For overlapping-trough objects (e.g. Fig. 3), are the column densities and covering factors of dense BAL gas higher in these objects (as indicated by high Fe II (optical)/[O III] ratios), or does the BAL gas just extend over a larger velocity range?
Last but not least, for our extremely reddened BAL quasars (e.g. Fig. 4) we will determine if the Balmer decrement gives the same $E(B-V)$ as the UV continuum, and pin down the long-wavelength end of the steeper-than-SMC extinction curves seen in some objects. Moreover, reddening of the broad emission lines and continuum provides important geometrical information, and dust, epecially in low-ionization BAL quasars, is important because it may be the signature of the birth cocoon of a newly emerging luminous quasar.

C) Telescope Justification: Our targets are faint enough to require a 4m-class telescope. NTT + SOFI is the only instrument/telescope combination available to us that can get the SNR (20-25 maximum in the bandpass of the blue or red grism) and resolution R ∼1000 that we require, in reasonable exposure times ranging from 15 minutes to 2 hours. In particular the broad and overlapping bandpasses of SOFI's blue and red grisms enable direct comparison of Hβ and Hα, and a determination of continuum spectral energy distributions, for our $z \sim 2$ quasars, as well as enabling a careful determination of the continuum underlying broad (3000 – 6000 km s^{-1} FWHM), blended Fe II and Hβ emission lines that can cover the whole of one atmospheric window.

D) Observing Mode Justification (visitor or service): We prefer visitor mode for the NTT because of the uncertain IR flux densities of some of these objects (due to reddening uncertainties and quasar variability – the latter of the order or <0.1-0.2mag). We would like to monitor the SNR in different wavelength regions in the SOFI bandpass and adjust exposure times if necessary, since our science requires high SNR for deblending.

E) Strategy for Data Reduction and Analysis: We will determine line ratios of Fe II, Hβ, [O III]$\lambda\lambda$4959, 5007, and Hα. We are experienced in using the IRAF SPECFIT package to deblend lines using an Fe II template method. The template is based on the identified Fe II lines in the narrow-lined Seyfert galaxy, I Zw 1 (e.g., Boroson & Green 1992, Vestergaard & Wilkes 2001). The largest source of uncertainty is continuum determination. Of particular importance is careful flux-density calibration over a wide wavelength range, because there are few continuum windows in quasar spectra. Usually the region around Hα is excellent, and near Hδ is possible. Another uncertainty is in the profile shape of Hβ, but an excellent approximation is provided by the relatively-isolated Hα profile. Our deblending should give errors on emission line measurements similar to the smaller half of those shown in Fig. 2 (for Fe II deblending, see Science Case).
We will relate the infrared properties with characteristics of the absorbing outflows deternined from our optical spectra. We have experience with photoionization codes needed for analyzing these data in this fashion.

REFERENCES

Becker et al. 2000, ApJ 538, 72
Boroson, T. A., & Green, R. F. 1992, ApJS, 80, 109
Ferrarese, L., & Merritt, D. 2000, ApJL, 539, 9
Hall, P. B. et al. 2002, ApJS, in press, astro-ph/0203252
Kaspi, S., et al. 2000, ApJ, 533, 631
Lacy, M., et al. 2001, ApJL, 551, L17
Laor, A. 2000, ApJ, 543, L111
McIntosh, D. H., et al. 1999, ApJ, 514, 40
Silk, J., & Rees, M. 1998, A&A, 331, L1
Boroson, T. A 2001, astro-ph/0109317
Fabian, A.C. 1999, MNRAS, 308, L39
Gebhardt, K., et al. 2000, ApJL, 539, 13
Hines, D., et al. 2001, ApJ, 563, 512
Kormendy, J., & Ho, L. 2000, Encyclopaedia A & A, in press
Laor, A. 1998, ApJ, 505, L83
Laor, A. 2001, ApJ, 553, 677
Menou, K., et al. 2001, ApJ, in press (astro-ph/0102410)
Voit, G., Weymann, R., & Korista, K. 1993, ApJ, 413, 95

8. Attachments (Figures)

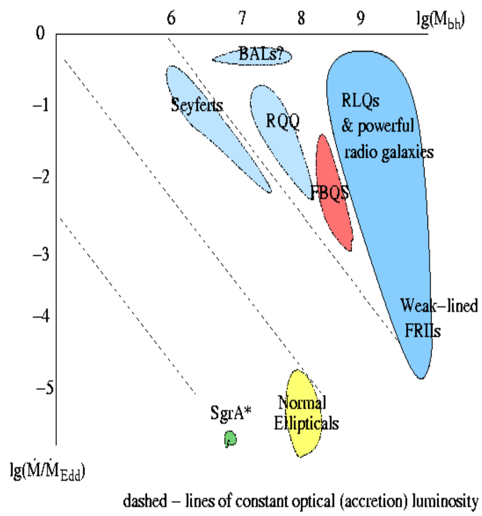

Fig. 1. M_{bh} vs. $\dot{M}/\dot{M}_{Edd}$ for low-redshift objects. Note the high M_{bh} of RLQs, and the high $\dot{M}/\dot{M}_{Edd}$ for low-redshift BALs (based on only three objects), compared to RQQs.

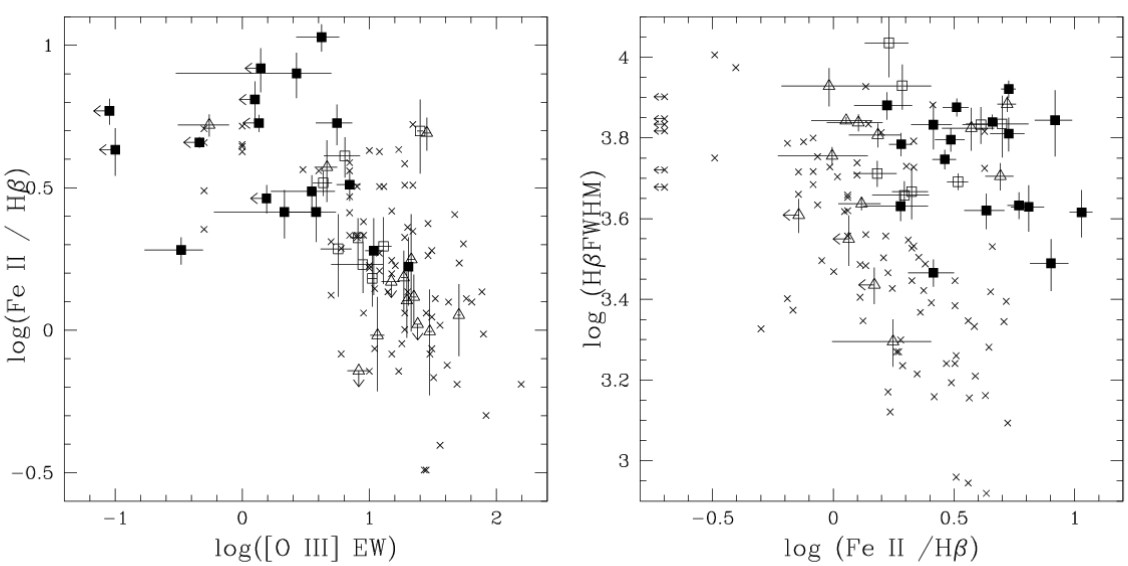

Fig. 2. **Left:** The anticorrelation between FeII and [O III] strength at low redshift (small x) from Boroson & Green (1992). Bright, high redshift normal BAL quasars (filled squares) extend the relationship to more extreme values, but the high redshift non-BAL quasars (open squares and triangles) occupy the same region as low redshift quasars. **Right:** Hβ width – FeII strength correlations for high and low redshift objects. High redshift objects have larger Hβ width on average, but even accounting for this by shifting the low-redshift correlation upwards, high redshift BAL quasars show larger Hβ width than expected for their FeII strength.

8. Attachments (Figures)

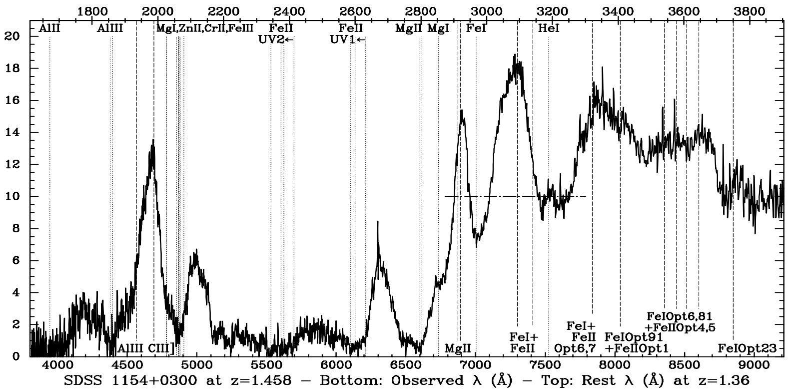

Fig.3: SDSS 1154+0300, an 'overlapping-trough' BAL quasar with broad troughs and hence a somewhat uncertain redshift.

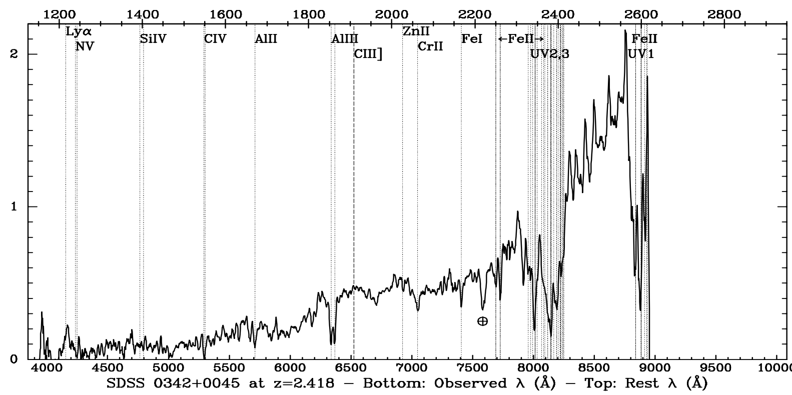

Fig.4: SDSS 0342+0045, an extremely reddened BAL quasar.

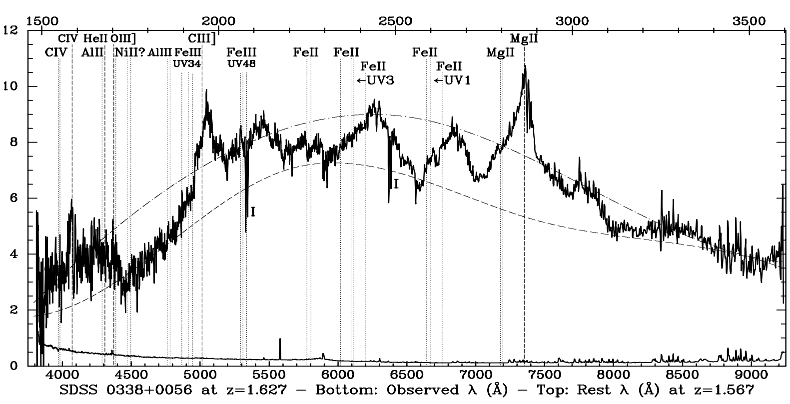

Fig.5: SDSS 0338+0056: BAL quasar or strong FeII emitter? The top curve shows a plausible unabsorbed continuum for a BAL interpretation; the bottom curve one for an FeII emitter interpretation.

9. Justification of requested observing time and lunar phase

Lunar Phase Justification: These near-IR observations can be done in bright time.

Time Justification: In order to determine line ratios of Fe II, Hβ, [O III]$\lambda\lambda$4959/5007 and Hα in our 15 targets, we need to deblend the overlapping features (see 'Strategy'). This requires profile information for the broad emission lines, and determination of relatively line-free continuum. To do this properly requires R $\sim$1000, full wavelength coverage over the Hβ and Hα regions, and continuum SNR $\sim$25 near Hβ and $\sim$20 near Hα. This resolution is expected to be sufficient to resolve the narrow [O III]$\lambda\lambda$4959/5007 emission lines, that are typically 500–700 km s^{-1} FWHM. (For our four lowest-redshift objects, information on Hβ will come from optical spectra already in hand.)
We determined J through K band flux densities by extrapolating our optical spectra, based on a Galactic reddening law and a standard composite quasar spectrum. We then used the SOFI and ISAAC ETCs, version 2.8.2, to estimate the exposure times required to reach the above SNR. We assumed a point source with a seeing of $0.8''$ and airmass 1.2, with a slit width of $0.6''$, with the blue or red grisms, as appropriate for coverage of Hβ and Hα. We also assumed instrumental overheads of 30% of the exposure times, 3 minutes for aquisition of each quasar and its atmospheric-absorption star (and occasional flux calibrators), with 3-4 minute exposures for each calibration star.
Including overhead, we require a total allocation of 16 hours with SOFI on NTT. Given the distribution on the sky of our objects, we request 1 night in Oct. and 1 night in Feb. For SNR$\sim$20 across Hα and Hβ for NIR-faintest target (not our faintest in SDSS z, but less reddened (bluer) than any of the targets fainter in z), we require 85 minutes of low-resolution spectroscopy with ISAAC in both H and K, at R$\sim$800 ($0.6''$ slit). Including overhead, we request 4 hours with ISAAC.

Calibration Request: Standard Calibration

10. Report on the last use of ESO facilities

67.A-0544 / P. Hall / Spectroscopy of Candidate Reddened Quasars from SDSS+2MASS

Telescope	Instrument	Obs. Dates	Completion (%)	Time lost (%)	Reason
NTT	EMMI	17-20 Apr 2001	100%	5%	technical

Current status of obtained data: paper-submitted

Remarks: No reddened quasars found, indicating that SDSS is very complete even for very reddened quasars (paper in preparation). Several candidates were carbon stars, to appear in Margon et al. (submitted). One highly reddened FIRST/2MASS quasar was found as well (Hall et al. in preparation). Observations of SDSS gravitational lens candidates also made to take advantage of excellent seeing; no lenses found, but one quasar binary and one quasar companion galaxy found (paper in preparation). Observations also made of the strange [OII]-without-[OIII] galaxy RCS 1443+0805 (paper in preparation).

11. Applicant's publications related to the subject of this application during the past two years

- Hall, P., *et al.* 2000, AJ, 120, 2220: Active Galactic Nuclei in the CNOC2 Field Galaxy Redshift Survey
- Hall, P., *et al.* 2001, to appear in Mass Outflow from AGN: New Perspectives, eds. Crenshaw, Kraemer & George (astro-ph/0107182): Extreme Broad Absorption Line Quasars from the Sloan Digital Sky Survey
- Hall, P., *et al.* 2002, ApJS in press (astro-ph/0203252): Unusual Broad Absorption Line Quasars from the Sloan Digital Sky Survey
- Hall *et al.* 2002, to be submitted: VLT Near-IR Spectroscopy and Polarimetry of Three Unusual SDSS Quasars
- Hall & Hutsemekers *et al.* 2002, to be submitted: VLT+UVES Spectroscopy of the Unusual BAL Quasars SDSS 0300+0048 and SDSS 1453+0029
- Hines, D., *et al.* [including Wills] 2001, ApJ, 563, 512: UV and Optical spectropolarimetry of IRAS QSOS: Dusty Scattering in Luminous Active Galactic Nuclei
- Menou, K., *et al.* [including Hall] 2001, ApJ, 561, 645: Broad Absorption Line Quasars in the Sloan Digital Sky Survey with VLA-FIRST Radio Detections
- Wills, Shang & Yuan 2000, New Astronomy Reviews 44, 511: H-beta line width and the UV-X-ray spectra of luminous AGN

12. List of targets proposed in this programme

Run	Target/Field	α	δ	Eq.	Mag.	Diam.	Additional info	Reference star
A	SDSS J2204+0031	22 04 45.26	+00 31 42.0	J2000	16.64		z=1.35; JH	
A	SDSS J2215−0045	22 15 11.94	−00 45 49.9	J2000	16.58		z=1.48; JH	
A	SDSS J0105−0033	01 05 40.75	−00 33 14.0	J2000	17.41		z=1.18; JH	
A	SDSS J0300+0048	03 00 00.57	+00 48 28.0	J2000	16.19		z=0.89; J	
A	SDSS J0318−0600	03 18 56.62	−06 00 37.7	J2000	16.81		z=1.97; HK	
A	SDSS J0338+0056	03 38 10.85	+00 56 17.6	J2000	18.43		z=1.63; JH	
A	SDSS J0342+0045	03 42 58.00	+00 45 39.1	J2000	19.39		z=2.42; HK	
B	SDSS J1125+0029	11 25 26.13	+00 29 01.3	J2000	17.75		z=0.87; J	
B	SDSS J1128+0113	11 28 28.31	+01 13 37.9	J2000	17.95		z=0.89; J	
B	SDSS J1154+0300	11 54 36.60	+03 00 06.4	J2000	17.48		z=1.46; JH	
B	SDSS J1214−0001	12 14 41.43	−00 01 37.9	J2000	18.57		z=1.04; J	
B	SDSS J1324−0217	13 24 44.11	−02 17 46.6	J2000	19.18		z=2.26; HK	
B	SDSS J1453+0029	14 53 33.01	+00 29 43.7	J2000	18.99		z=1.30; JH	
B	SDSS J1456+0114	14 56 03.08	+01 14 45.5	J2000	18.62		z=2.36; HK	
C	SDSS J0149−0114	01 49 05.28	−01 14 04.9	J2000	18.78		z=2.10; HK	

Target Notes: All magnitudes are SDSS z' magnitudes, closest to the near-IR. Under Additional info, the redshift is given, followed by the near-IR bandpass(es) in which we need to acquire spectra to cover Hβ and Hα (only the latter for the lowest redshift targets). Spectra of all targets can be seen in Hall et al. (2002).

13. Scheduling requirements

14. Instrument configuration

Telescope	Instrument	Parameter	Value or list
UT1	ISAAC	SWS-LR	1.625 microns, 2.2 microns
NTT	SOFI	Spectroscopy-long-slit	Blue Grism
NTT	SOFI	Spectroscopy-long-slit	Red Grism